

## Rare $b$ -hadron decays at LHCb

---

**Luis Miguel Garcia Martin**<sup>\*†</sup>

*IFIC (CSIC-Universitat de València)*

*E-mail:* [lgarciam@cern.ch](mailto:lgarciam@cern.ch)

Rare  $b$ -hadron decays are sensitive probes of New Physics, as new particles can give significant contributions on physics observables. Searches for phenomena beyond the Standard Model are focused on the study of branching fractions, CP asymmetries and angular observables of rare  $b$ -hadron decays. During Run 1 and Run 2 of the LHC, the LHCb experiment has collected large samples of these kind of decays. The latest measurements help to constrain the size of right-handed currents in extensions of the Standard Model.

*European Physical Society Conference on High Energy Physics - EPS-HEP2019 -  
10-17 July, 2019  
Ghent, Belgium*

---

<sup>\*</sup>Speaker.

<sup>†</sup>On behalf of the LHCb collaboration.

## 1. Introduction

Rare  $b$ -hadron decays involve Flavor-Changing Neutral-Currents (FCNC), which are forbidden at tree level within the Standard Model (SM) and, thus, are very suppressed. Due to this, they are sensitive to New Physics (NP), which involve new particles and affect the transition dynamics, as shown in Figure 1. Many models of NP [1, 2] predicts significant changes in the measured value

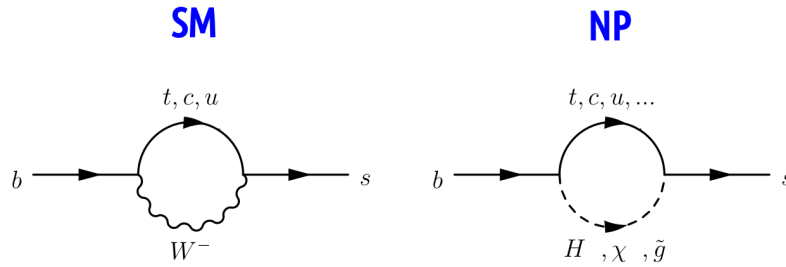


**Figure 1:** Feynman diagram of the FCNC  $b \rightarrow s\gamma$  transition in the SM (left) and with NP contributions (right).

of the related observables due to these interferences. Furthermore, the study of new particles entering in the loop grants access to much larger energy scales than those achieved with direct searches. As a consequence, rare  $b$ -hadron decays are an unique tool to test the SM and to study the physics beyond it.

These decays are described using a model-independent approach by the Effective Operator Product expansion:

$$\mathcal{H}_{eff} = -4 \frac{G_F}{\sqrt{2}} V_{CKM} \sum_i (C_i O_i + C'_i O'_i), \quad (1.1)$$

where  $C_i^{(\prime)}$  are effective couplings named Wilson coefficients, which describes the short-distance effects and  $O_i^{(\prime)}$  are local operators encoding long-distance contributions. The primed terms ( $C'_i$  and  $O'_i$ ) refers to right-handed currents, whereas the left-handed currents are portrayed by the other terms ( $C_i$  and  $O_i$ ). The SM provides a predicted value for the Wilson coefficients which can be compared with the one extracted from global fits. Since the charged current interactions are left-handed in the SM, the right-handed currents are suppressed. Therefore, the predicted value for the  $C'_i$  parameters is close to zero. Rare  $b$ -hadron decays are described by  $O_7^{(\prime)}$ ,  $O_9^{(\prime)}$  and  $O_{10}^{(\prime)}$  operators. The former represent radiative penguin transition ( $b \rightarrow s\gamma$ ), whereas the other two rule the  $b \rightarrow sll$  transitions.

Recently, tensions with respect to the SM have appeared in several decays with a  $b \rightarrow sll$  transition. These deviations have been observed in branching ratio measurements, like in the  $B \rightarrow K^{(*)} \mu^+ \mu^-$  decay [3], although they are affected by large theoretical uncertainties from the determination of the form factors. Similar deviations have been found in angular analyses [4] and Lepton Flavour Universality tests [5], which provide theoretically precise observables. Moreover, there are two very recent results of analyses including the  $b \rightarrow s\gamma$  transition, which provide further constraints to the value of the  $C'_7$  coefficient. These results will be presented in Sections 2 and 3, and they open the door to new observables discussed in Section 4.

## 2. Measurement of CP-violating observables in $B_s^0 \rightarrow \phi \gamma$

The photon polarization can be accessed in the  $B_s^0 \rightarrow \phi \gamma$  decay by exploiting the mixing induced interference in the time-dependent decay rate:

$$\Gamma(t) \propto e^{-\Gamma_s t} \left[ \cosh\left(\frac{\Delta\Gamma_s t}{2}\right) - A_{\phi\gamma}^\Delta \sinh\left(\frac{\Delta\Gamma_s t}{2}\right) \pm C_{\phi\gamma} \cos(\Delta m_s t) \mp S_{\phi\gamma} \sin(\Delta m_s t) \right]. \quad (2.1)$$

The  $A_{\phi\gamma}^\Delta$  and  $S_{\phi\gamma}$  parameters are sensitive to the photon polarization, while the  $C_{\phi\gamma}$  is related to the direct CP violation. The SM predicts these parameters to have value close to zero [6]. The sign of the last two terms depends on whether the produced particle is a  $B_s^0$  or a  $\overline{B}_s^0$ . Therefore, the flavor of the particle needs to be tagged to access these terms. A previous analysis used data collected at LHCb during the Run 1 of the LHC with no information about the flavor of the initial particle, measuring for first time ever  $A_{\phi\gamma}^\Delta = -0.98^{+0.46+0.23}_{-0.52-0.20}$  [7].

In a recent analysis using the same dataset, the measurement is updated [8] including flavor information via flavor tagging. The decay-time acceptance is modelled using the  $B^0 \rightarrow K^{*0} \gamma$  decay, which has a similar topology. The sPlot technique [9] is used to subtract the background in the physical and control channels, which allows to derive the signal decay time from the mass fit. The result of the mass fit is shown in Figure 2.

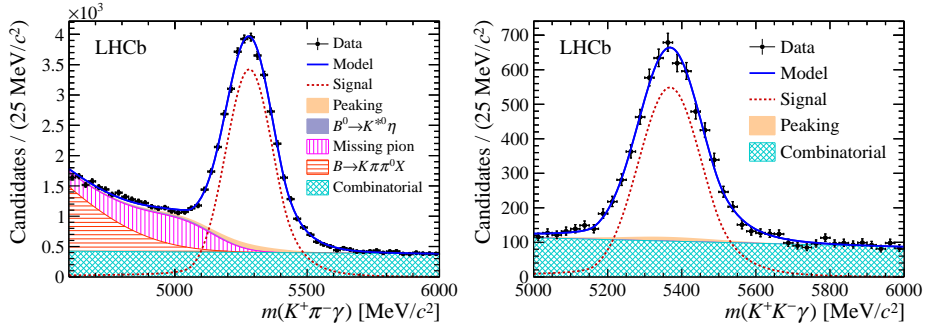


**Figure 2:** Invariant mass distribution of the  $B_s^0 \rightarrow \phi \gamma$  (left) and  $B_s \rightarrow K^{*0} \gamma$  (right) candidates. The result of an unbinned maximum likelihood fit is shown by a blue curve.

The value of the  $A_{\phi\gamma}^\Delta$ ,  $S_{\phi\gamma}$  and  $C_{\phi\gamma}$  parameters is extracted separately for events tagged as  $B_s^0$ ,  $\overline{B}_s^0$  and with no tagging information. For this purpose, a simultaneous unbinned maximum likelihood fit to the decay-time distribution of the signal and control channels is used, which is shown in Figure 3. The measured values are:

$$\begin{aligned} S_{\phi\gamma} &= 0.43 \pm 0.30 \pm 0.11, \\ C_{\phi\gamma} &= 0.11 \pm 0.29 \pm 0.11, \\ A_{\phi\gamma}^\Delta &= -0.67^{+0.37}_{-0.41} \pm 0.17, \end{aligned} \quad (2.2)$$

where the first uncertainty is statistical, which has been lowered by improving the reconstruction with respect to the previous analysis, and the second uncertainty is systematic. These values are compatible with the SM model predictions. This analysis provides the first measurement of the  $S_{\phi\gamma}$  and  $C_{\phi\gamma}$  in the  $B_s^0$  decays, which is competitive with previous results achieved in B-factories using  $B^0$  decays [10, 11].

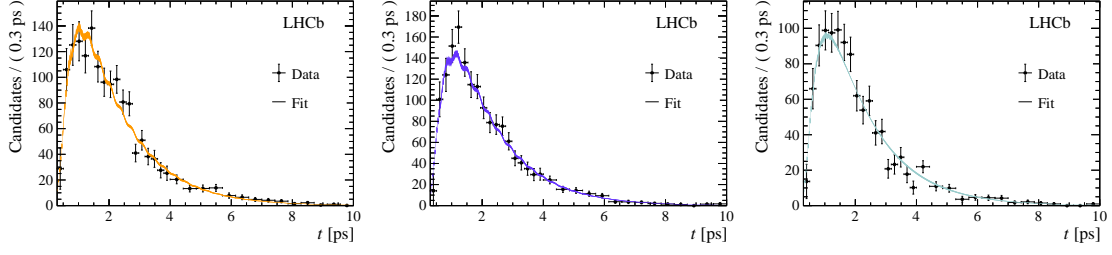


**Figure 3:** Decay time distributions for  $B_s^0 \rightarrow \phi \gamma$  candidates where the event is tagged as  $B_s^0$  (left),  $\overline{B}_s^0$  (center) and with no tagging information (right). The result of a simultaneous unbinned maximum likelihood fit is shown by a blue curve.

### 3. First observation of $\Lambda_b^0 \rightarrow \Lambda^0 \gamma$

The SM predicts the branching ratio for the  $\Lambda_b^0 \rightarrow \Lambda^0 \gamma$  decay to be in the range  $[10^{-7} - 10^{-5}]$  [12]. This decay has never been observed and the best limit to its branching ratio was set by CDF at  $B(\Lambda_b^0 \rightarrow \Lambda^0 \gamma) < 1.9 \times 10^{-3}$  at 95% CL [13].

Recently, the LHCb collaboration has performed a search for this decay using data collected in 2016, corresponding to an integrated luminosity of  $1.7 \text{ fb}^{-1}$  [14]. The reconstruction of this decay channel is quite challenging at LHCb due to two factors. On the one hand, the photon is reconstructed solely as a cluster in the electromagnetic calorimeter and, thus, its direction is not known. On the other hand, the  $\Lambda^0$  travels a long distance before decaying due to its large life-time. As a consequence, there is no information about the  $\Lambda_b^0$  decay vertex, which allows huge contributions from prompt background. A high performance BDT is used to reject signal from combinatorial background. Finally, neutral particle identification tools are exploited to reject potential background due to  $\pi^0$  misidentified as  $\gamma$ .

The branching ratio is extracted by using the  $B^0 \rightarrow K^{*0} \gamma$  decay as a normalization channel. A simultaneous unbinned maximum likelihood fit to the mass distribution of the signal and normalization channels is performed, and its results are shown in Figure 4. A clear signal peak of  $65 \pm 13$

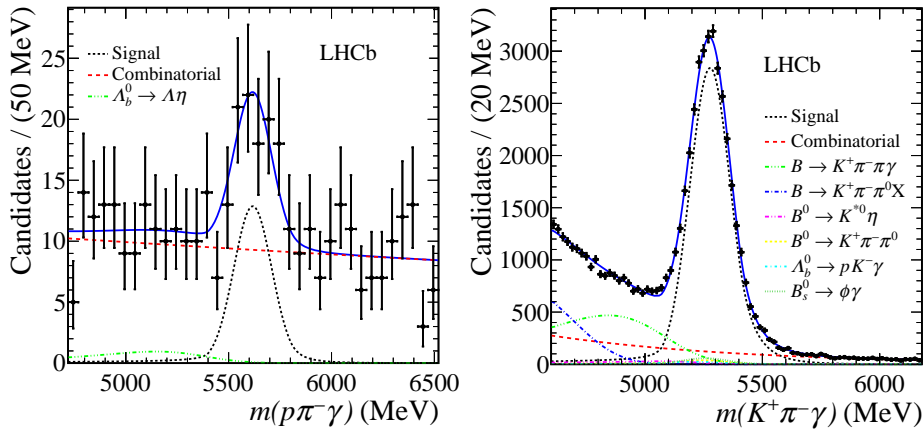


**Figure 4:** Invariant mass distribution of the  $\Lambda_b^0 \rightarrow \Lambda^0 \gamma$  (left) and  $B^0 \rightarrow K^{*0} \gamma$  (right) candidates. The result of a simultaneous unbinned maximum likelihood fit is shown by a blue curve.

$\Lambda_b^0 \rightarrow \Lambda^0 \gamma$  events is found with a significance of  $5.6\sigma$ , representing the first observation ever of a radiative  $b$ -baryon decay. The branching ratio is measured to be:

$$B(\Lambda_b^0 \rightarrow \Lambda^0 \gamma) = (7.1 \pm 1.5 \pm 0.7) \times 10^{-6}, \quad (3.1)$$

where the first uncertainty is statistical, the second is systematic and the last one comes from external measurements and is dominated by the ratio of hadronization fractions.

#### 4. Sensitivity to the photon polarization in $b$ -baryon decays

The study of  $b$ -baryon decays grant direct access to the photon polarization asymmetry ( $\alpha_\gamma$ ) [15] and, thus, to the helicity of the  $b \rightarrow s \gamma$  process. The SM prediction for this observable is  $\alpha_\gamma \simeq 1$  [16], i.e. the photon is predicted to be polarized mainly left-handed. The feasibility of this measurement is tested using simulated  $\Lambda_b^0 \rightarrow \Lambda^0 \gamma$  and  $\Xi_b^- \rightarrow \Xi^- \gamma$  decays. The photon polarization is extracted from the angular distributions using the helicity formalism, which for  $\Lambda_b^0 \rightarrow \Lambda^0 \gamma$  is:

$$\Gamma_{\Lambda_b}(\theta_p) = \frac{1}{4} \left( 1 - \alpha_\gamma \alpha_\Lambda \cos \theta_p \right), \quad (4.1)$$

whereas for  $\Xi_b^- \rightarrow \Xi^- \gamma$  is:

$$\Gamma_{\Xi_b}(\theta_\Lambda, \theta_p) = \frac{1}{4} \left( 1 - \alpha_\gamma \alpha_\Xi \cos \theta_\Lambda + \alpha_\Lambda \cos \theta_p \left( \alpha_\Xi - \alpha_\gamma \cos \theta_\Lambda \right) \right). \quad (4.2)$$

The helicity angles are  $\theta_p$  and  $\theta_\Lambda$ , and the  $\alpha_\Xi$  and  $\alpha_\Lambda$  parameters are taken from the PDG [17]. The statistical sensitivity to the photon polarization as a function of the number of candidates is studied using Monte Carlo toys. This study, depicted in Figure 5, shows a similar sensitivity for both channels.

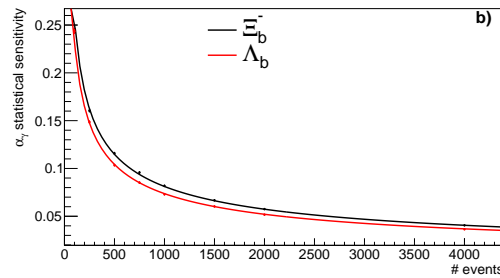


**Figure 5:** Statistical sensitivity to the photon polarization as a function of the number of reconstructed events for the  $\Lambda_b^0 \rightarrow \Lambda^0 \gamma$  (red) and  $\Xi_b^- \rightarrow \Xi^- \gamma$  (black) decays.

The reconstruction and backgrounds are modelled via a modified angular distribution:

$$\Gamma(\theta_p) = \left( f_S(\theta) \times A(\theta) \right) * R(\theta) + \frac{S}{B} \left( f_B(\theta) \right), \quad (4.3)$$

where  $f_S$  is the theoretical angular distribution,  $R$  describes the angular resolution,  $A$  represents the angular acceptance and  $f_B$  is the angular background distribution expected from combinatorial

background. The ratio between the signal and the background yield is represented with the S/B parameter. Each of these effects are tested independently in the following.

The effect of the angular resolution and acceptance on the photon polarization is tested with 1000 pseudoexperiments, where the number of candidates is fixed to 1000 to focus on the reconstruction effects instead of on statistical ones. This study concludes that the effect of the resolution is negligible, while the effect of the acceptance is asymmetric in  $\alpha_\gamma$ , as shown in Figure 6.

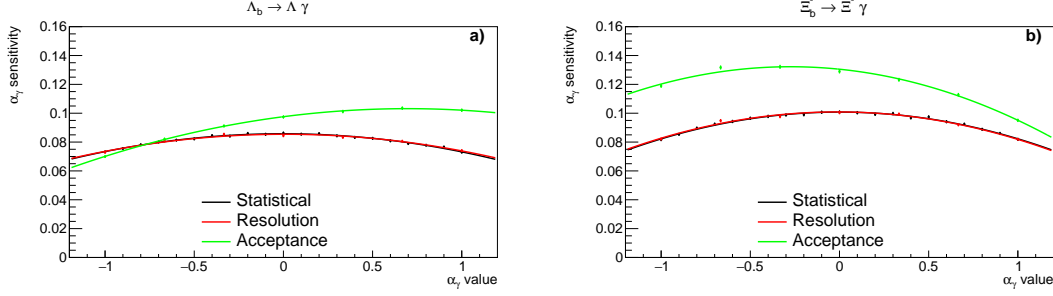


**Figure 6:** Sensitivity to the photon polarization as a function of its value for the  $\Lambda_b^0 \rightarrow \Lambda^0 \gamma$  (left) and  $\Xi_b^- \rightarrow \Xi^- \gamma$  (right) decays, including statistical (black), angular resolution (red) and angular acceptance (green) effects.

Lastly, the background contribution effect is studied as a function of S/B. This is achieved by generating and fitting 1000 dataset with 1000 signal candidates and varying the background yield. Additionally, different background shapes are tested to fully understand its contribution to the photon polarization sensitivity. As it can be observed in Figure 7, a high S/B is important to achieve a good accuracy in the measurement of the photon polarization. Moreover, the different background shapes tested contribute with a similar dilution to the photon polarization.

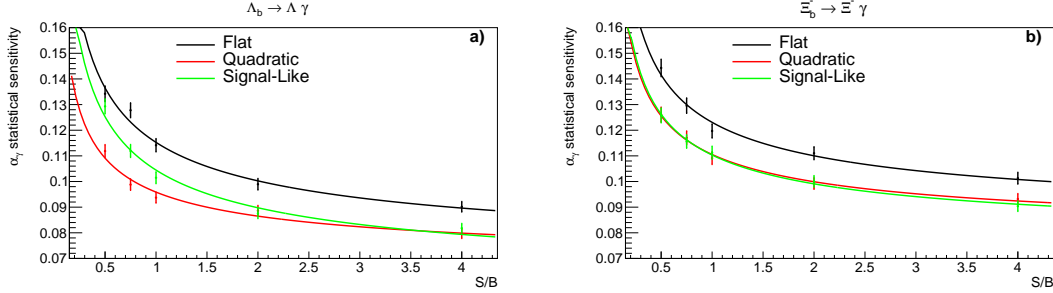


**Figure 7:** Sensitivity to the photon polarization as a function of the signal over background ratio for the  $\Lambda_b^0 \rightarrow \Lambda^0 \gamma$  (left) and  $\Xi_b^- \rightarrow \Xi^- \gamma$  (right) decays, including the effects of background with different shapes.

## 5. Summary

Rare  $b$ -hadron decays are excellent probes of NP since they allow to test large energy scales via indirect searches. Several deviations with respect to the SM have been observed in recent results from studies involving the  $b \rightarrow sll$  transition performed at the LHCb. Besides, the LHCb has provide two recent measurement involving  $b \rightarrow s\gamma$  transitions. On the one hand, The  $C_{\phi\gamma}$  and

$S_{\phi\gamma}$  have been measured for the first time in the  $B_s^0 \rightarrow \phi\gamma$  decay. Additionally, the measurement of the  $A_{\phi\gamma}^\Delta$  parameter has been updated with higher number of reconstructed candidates. On the other hand, LHCb has provide the first observation of a radiative  $b$ -baryon decay observing 65 candidates of the  $\Lambda_b^0 \rightarrow \Lambda^0\gamma$  decay. This has open the possibility to perform a measurement of the photon polarization in radiative  $b$ -baryon decays. These results provide constraint to the  $C_7'$  coefficient, helping to narrow the search for NP sources.

## References

- [1] L. Everett et al., Alternative approach to  $b \rightarrow s\gamma$  in the  $\mu$ MSSM, *J. High Energ. Phys.* (2002), 2002: 022.
- [2] F. Yu, E. Kou, and C. Lu, Photon polarization in the  $b \rightarrow s\gamma$  processes in the left-right symmetric model, *J. High Energ. Phys.* (2013), 2013: 102.
- [3] R. Aaij et al. (LHCb Collaboration), Differential branching fractions and isospin asymmetries of  $B \rightarrow K(*)\mu^+\mu^-$  decays, *J. High Energ. Phys.* (2014) 2014: 133.
- [4] R. Aaij et al. (LHCb Collaboration), Angular analysis of the  $B^0 \rightarrow K^{*0}\mu^+\mu^-$  decay using  $3 \text{ fb}^{-1}$  of integrated luminosity, *J. High Energ. Phys.* (2016) 2016: 104.
- [5] R. Aaij et al. (LHCb Collaboration), Test of Lepton Universality Using  $B^+ \rightarrow K^+\ell^+\ell^-$  Decays, *Phys. Rev. Lett.* 113, 151601
- [6] F. Muheim, Y. Xie, R. Zwicky, Exploiting the width difference in  $B_s \rightarrow \phi\gamma$ , *Phys. Lett. B* 664 (2008), pp. 174–179.
- [7] R. Aaij et al. (LHCb Collaboration), First Experimental Study of Photon Polarization in Radiative  $B_s^0$  Decays, *Phys. Rev. Lett.* 118, 021801.
- [8] R. Aaij et al. (LHCb Collaboration), Measurement of  $CP$ -Violating and Mixing-Induced Observables in  $B_s^0 \rightarrow \phi\gamma$  Decays, *Phys. Rev. Lett.* 123, 081802.
- [9] M. Pivk and F. R. Le Diberder. SPlot: A Statistical tool to unfold data distributions, *Nucl. Instrum. Meth. A* 555 (2005), pp. 356-369.
- [10] BaBar Collaboration, Measurement of time-dependent  $CP$  asymmetry in  $B^0 \rightarrow K_s^0\pi^0\gamma$  decays, *Phys. Rev. D* 78 (2008).
- [11] Belle Collaboration, Time-dependent  $CP$  asymmetries in  $B^0 \rightarrow K_s^0\pi^0\gamma$  transitions, *Phys. Rev. D* 74 (2006), p. 111104.
- [12] Y. Wang, Y. Li, and C. Lu, Rare Decays of  $\Lambda_b^0 \rightarrow \Lambda^0\gamma$  and  $\Lambda_b^0 \rightarrow \Lambda^0 l^+ l^-$  in the Light-cone Sum Rules, *Eur. Phys. J. C* 59 (2009) 861.
- [13] D. Acosta et al. (CDF Collaboration), Search for radiative  $b$ -hadron decays in  $p\bar{p}$  collisions at  $\sqrt{s} = 1.8\text{TeV}$ , *Phys. Rev. D* 66, 112002.
- [14] R. Aaij et al. (LHCb Collaboration), First Observation of the Radiative Decay  $\Lambda_b^0 \rightarrow \Lambda\gamma$ , *Phys. Rev. Lett.* 123, 031801.
- [15] Garcia Martin, L.M., Jashal, B., Martinez Vidal, F. et al., Radiative  $b$ -baryon decays to measure the photon and  $b$ -baryon polarization, *Eur. Phys. J. C* (2019) 79: 634.
- [16] B. Grinstein et al., Photon polarization in  $B \rightarrow X\gamma$  in the standard model, *Phys. Rev. D* 71 (1 Jan. 2005), p. 011504.
- [17] M. Tanabashi et al. (Particle Data Group), *Phys. Rev. D* 98, 030001 (2018).